Thermodynamics of HMGB1 Interaction with Duplex DNA†

Susanne Müller,‡ Marco E. Bianchi,‡ and Stefan Knapp*,§

DIBIT, San Raffaele Scientific Institute, via Olgettina 58, 2032 Milano, Italy, and Pharmacia & Upjohn, Discovery Research Oncology, Department of Structural Chemistry, Viale Pasteur 10, 20014 Nerviano, Italy

Received January 16, 2001; Revised Manuscript Received May 29, 2001

ABSTRACT: The high mobility group protein HMGB1 is a small, highly abundant protein that binds to DNA in a non-sequence-specific manner. HMGB1 consists of 2 DNA binding domains, the HMG boxes A and B, followed by a short basic region and a continuous stretch of 30 glutamate or aspartate residues. Isothermal titration calorimetry was used to characterize the binding of HMGB1 to the double-stranded model DNAs poly(dAdT)·(dTdA) and poly(dGdC)·(dCdG). To elucidate the contribution of the different structural motifs to DNA binding, calorimetric measurements were performed comparing the single boxes A and B, the two boxes plus or minus the basic sequence stretch (AB_{bt} and AB), and the full-length HMGB1 protein. Thermodynamically, binding of HMGB1 and all truncated constructs to duplex DNA was characterized by a positive enthalpy change at 15 °C. From the slopes of the temperature dependence of the binding enthalpies, heat capacity changes of -0.129 ± 0.02 and -0.105 ± 0.05 kcal mol^{-1} K^{-1} were determined for box A and full-length HMGB1, respectively. Significant differences in the binding characteristics were observed using full-length HMGB1, suggesting an important role for the acid tail in modulating DNA binding. Moreover, full-length HMGB1 binds differently these two DNA templates: binding to poly(dAdT)·(dTdA) was cooperative, had a larger apparent binding site size, and proceeded with a much larger unfavorable binding enthalpy than binding to poly(dGdC)·(dCdG).

HMG box proteins are all characterized by the presence of a DNA binding domain of the HMG box type (*1*−*3*). While one branch of this family is composed of sequence-specific DNA binding proteins such as the transcription factor lymphoid enhancer factor-1 (LEF1) (*4*) or the sex determining factor SRY (*5*), another branch of the family, encompassing the chromosomal proteins HMGB1 and -2, binds to DNA in a non-sequence-specific manner (*6*). [HMGB1 was previously known as HMG1 (*7*).] The HMGB1 protein contains 2 homologous DNA binding domains, the HMG boxes A and B, each around 75 amino acids in length, connected by a short linker region and followed by a stretch of basic amino acids. The C-terminus is highly negatively charged, consisting of a continuous stretch of 30 glutamate or aspartate residues.

The two HMG boxes of HMGB1 show an identity of only 29% on the amino acid level. However, the global fold of the HMG box is well conserved and is composed of three alpha helices (I−III) arranged in an L-like shape and stabilized by two hydrophobic cores, as determined by structural studies using single HMG boxes (*8*). Several structural and functional differences between the two HMG boxes in HMGB1 have been observed. In particular, the degree of bending introduced into DNA upon binding is higher for box B, and binding affinities to four-way junctions differ between the two boxes (reviewed in *8, 9*). Binding to four-way junctions occurs in an asymmetric fashion, with box A binding in a structure-specific manner to the center of the junction, whereas box B makes contacts along one of the double-stranded arms (*10, 11*). In the context of the full-length protein, calorimetric data have shown that box A and box B behave as independent domains and do not interact with each other. However, interactions occur between the acidic tail and one of the boxes (*12*). In addition, the acidic tail reduces DNA binding affinity and supercoiling ability (*13, 14*).

High-affinity binding of HMGB1 has been demonstrated to DNA with highly bent structures. Four-way junctions and other distorted DNA structures such as cisplatin-modified DNA are bound with dissociation constants in the range of 10^{-8}−10^{-9} M (*15*−*17*), and a functional role of HMGB1 potentially consistent with the binding to cruciform DNA has been demonstrated for VDJ recombination (*18, 19*). In addition, HMGB1 itself induces structural distortion into double-stranded DNA, as shown by circularization assays (*20*).

Considering the high abundance of HMGB1 in the cell, other DNA species than the rarely occurring distorted forms of DNA must serve as binding sites for HMGB1. Indeed, HMGB1 has been shown to interact with and increase binding of several transcription factors, like the Hox proteins, the steroid hormone receptors, p53, and TBP (reviewed in *2*). The physical interaction with HMGB1 enhances the ability of the partner proteins to bind to their cognate target sites, without altering their sequence specificity. The functional importance of HMGB1 as a regulator of transcription has been confirmed by the phenotype of the HMGB1

† This work was supported by the Italian Association for Cancer Research (AIRC), by MURST Progetti di Rilevante Interesse Nazionale, and by the European Union (Grant ERBFMRX CT 97 0109). S.M. is a trainee in the Training and Mobility of Researchers program.

* Author to whom correspondence should be addressed. Tel: +39 02 4838 5072. Fax: +39 02 4838 3965. E-mail: stefan.knapp@eu.pnu.com.

‡ San Raffaele Scientific Institute.

§ Pharmacia & Upjohn.

10.1021/bi0100900 CCC: $20.00
Published on Web 08/03/2001

knockout mouse, which dies shortly after birth due to hypoglycemia and shows a defect in the transcriptional enhancement of the glucocorticoid receptor (*21*).

Despite a large amount of knowledge concerning the binding of HMGB1 to discrete structured DNA motifs (reviewed in *8*), the binding characteristics of HMGB1 to linear duplex DNA in solution have been poorly characterized so far, probably due to the inherent difficulties in assaying nonspecific DNA binding. Structural information of the HMGB1-like proteins in *Drosophila* (HMG-D) and yeast (NHP6A) recently gave insight into the molecular aspects of HMG box binding to unmodified linear duplex DNA (*9*, *22*). However, the binding properties of full-length HMGB1, as opposed to individual boxes, are still incompletely understood. Indeed, the function of the acidic tail is still unclear as well as why mammalian HMGB1 and related proteins contain two HMG boxes while *Drosophila* and yeast HMGB1-like proteins contain only a single box.

In this study, we used isothermal titration calorimetry (ITC)[1] to characterize the thermodynamic aspects of HMGB1 binding to double-stranded DNA. ITC offers a direct method to study binding properties in solution by measuring heat effects upon association of a ligand with its binding partner and is the method of choice to study the thermodynamics of molecular association in solution. To determine the significance of the presence of two HMG boxes in HMGB1, we compared measurements on the full-length protein with the binding of single boxes A and B and of HMGB1 without the acidic tail (AB). The binding characteristics of full-length HMGB1 differ significantly from those of single boxes, which are frequently used as models to characterize binding of the complete HMGB1 protein. Most importantly, a protein consisting of the two HMG boxes but missing the acidic tail does not reflect the binding characteristics of the full-length protein, suggesting an important role of the acidic tail in modulating DNA binding properties. Moreover, the complete protein binds poly-AT with different binding characteristics and affinities as compared to poly-GC, suggesting that HMGB1 can adopt different modes of DNA binding.

MATERIALS AND METHODS

Cloning, Expression, and Purification of Proteins. The plasmids pRNHMG1/M1-V176 to express HMGB1 (AB), pT7-HMG1bA encoding box A, and pT7-HMG1bB encoding box B have been described elsewhere (*23*). The plasmid pT7-7-rHMG1cm encoding the full-length HMGB1 protein was a kind gift of Prof. J. O. Thomas (Cambridge). The construct pT7-HMGB1 AB_{bt}, encoding amino acids 1−187, was created by replacing the *Nsi*I−*Hin*dIII fragment of the plasmid pT7-RNHMG1 (*24*) with a PCR product between the primer pair 5′-CATATGCATTCTTTGTGCAAACCT-3′ and 5′-CCCCAAGCTTATTCCTTCTTTTTCTTG CTC-3′, cut with *Nsi*I and *Hin*dIII. The structure of the construct was verified by nucleotide sequencing. Expression and purification of the single boxes and HMGB1 (AB) were performed as described previously, and HMGB1 AB_{bt} was purified accordingly (*23*). For the full-length protein, a freshly transformed colony was used to inoculate an overnight culture grown in M9 medium complemented with 20 g/L casamino acids, 0.5% glycerol, 5 g/L yeast extract, 0.4% glucose, and 100 μg/mL chloramphenicol. Three hundred milliliters of the overnight culture was than used to inoculate a 3 L culture in an ADI 7 l autoclavable bioreactor (Applikon). At an optical density OD_{595} of 0.7, IPTG was added to the culture to a final concentration of 0.5 mM. Shaking was reduced to 150−200 rpm and growth temperature to 23 °C. Growth was continued for another 16 h. The protein was processed as described above, and we obtained 25 mg of pure full-length HMGB1. Protein concentrations were determined spectroscopically using the method of Gill and Hippel (*25*). The following extinction coefficients were used for the native protein: box A, $\epsilon_{280} = 9.98 \times 10^3$ M^{-1} cm^{-1}; box B, $\epsilon_{280} = 1.15 \times 10^4$ M^{-1} cm^{-1}; AB, AB_{bt}, and full-length HMGB1, $\epsilon_{280} = 2.14 \times 10^4$ M^{-1} cm^{-1}.

CD Spectroscopy. CD spectra were recorded using a J-710 (Jasco) spectropolarimeter and software provided by the manufacturer. Cuvettes with a 0.5 cm path length were used. Each spectrum was averaged using 4 accumulations and a scan speed of 20 nm/min. Identical buffers were used in CD and ITC experiments.

Isothermal Titration Calorimetry. Calorimetric measurements were carried out at constant temperatures using a VP-ITC titration calorimeter from MicroCal Inc., Northampton, MA. Samples were extensively dialyzed against the buffer used (50 mM Hepes, pH 7.5, 100 mM NaCl, 1 mM DTT). All solutions were carefully degassed before the titrations using equipment provided with the calorimeter. Each titration experiment consisted of a first (5 μL) injection followed by 10 μL injections. Heats of dilution were measured in blank titrations by injecting the ligand (protein in reverse titrations or DNA in titrations) into the buffer used in the particular experiment and were subtracted from the binding heats. The double-stranded nucleic acids poly(dAdT)·(dTdA) and poly(dGdC)·(dCdG) were purchased from Pharmacia and used without additional purification. DNA concentrations were determined spectrophotometrically using the extinction coefficients provided by the manufacturer: poly(dAdT)·(dTdA), $\epsilon_{260} = 13\,200$ M^{-1} (base pair)$^{-1}$ cm^{-1}; poly(dGdC)·(dCdG), $\epsilon_{260} = 16\,800$ M^{-1} (base pair)$^{-1}$ cm^{-1}. Poly(dAdT)·(dTdA) had an average length of 5 kb and poly(dGdC)·(dCdG) of 0.9 kb.

Binding isotherms were evaluated using a model for binding of noninteracting ligands to a lattice of ligand binding sites (*26*).

$$\upsilon/L = K_B(1 - n\upsilon)\left[\frac{1 - n\upsilon}{1 - (n-1)\upsilon}\right]^{n-1} \quad (1)$$

The equation is in the Scatchard form where υ represents the fractional occupancy of the lattice $[HMGB1]_{bound}$/[DNA base pairs] and $L = [HMGB1]_{free}$. K_B is the association constant and n is the number of base pairs covered by each ligand. The reaction heat Q_i in the calorimetrically sensed solution volume V_o at a particular value of υ_i is

$$Q_i = \upsilon_i[DNA_{base\ pair}]\Delta H^\circ_{obs} V_o \quad (2)$$

where $\Delta Q(i)$ is the observed enthalpy of binding sensed by the calorimeter by the ith injection (ΔQ_i). Corrections were made for the displacement of solution in the calorimetrically

[1] Abbreviations: ITC, isothermal titration calorimetry; poly-AT, poly(dAdT)·(dTdA); poly-GC, poly(dGdC)·(dCdG).

sensed cell by each injection assuming fast mixing and kinetics according to

$$\Delta Q(i) = Q(i) + \frac{V_i}{V_o}\left[\frac{Q(i) + Q(i-1)}{2}\right] - Q(i-1) \quad (3)$$

where $\Delta Q(i)$ is the heat release as a result of the ith injection and V_i is the injection volume. The equilibrium parameters K_{obs}, n_{obs}, and ΔH°_{obs} were determined using nonlinear least-squares fits of the binding isotherm (eq 3) to the observed heats using routines available within the Mathematica program package (Wolfram Research), where the heat release of the ith injection (Q_i) was calculated using eq 2 and the fractional occupancy of the lattice (υ_i) was calculated from eq 1. Errors in the equilibrium parameters were determined by comparing the fitted parameters of at least two independent titration experiments for each experimental condition. Changes in the free energy (ΔG_{obs}) and entropy ($-T\Delta S_{obs}$) upon binding were calculated from determined equilibrium parameters using

$$-RT\ln(K_{obs}) = \Delta G_{obs} = \Delta H_{obs} - T\Delta S_{obs} \quad (4)$$

Thermodynamic parameters determined in this study are valid only under the specified solution condition, which is indicated by the subscript "obs" throughout the paper.

Selection of the Binding Model. The theoretical background for the binding of nonspecific DNA binding proteins to large double-stranded DNA molecules has been described for both noncooperative and cooperative binding (*26*, *27*). Binding isotherms measured using the single boxes A and B as well as AB and AB_{bt} could be readily interpreted using a noncooperative binding model. We were unable to improve the quality of the fit using a model in which a cooperativity parameter was included (*26*). Therefore, we concluded that there is no justification using a more complex fitting model. Also data measured on full-length HMGB1 to poly-GC could be fitted using a noncooperative binding model. However, binding isotherms recorded using full-length HMGB1 and poly-AT indicated a more complex binding behavior: In this case, binding isotherms showed additional heat effects at high saturation levels of the duplex DNA, indicating cooperativity. However, we were unable to obtain improved fits of these data using a cooperative binding model with a cooperativity parameter $\omega \neq 1$. It is therefore probable that the observed additional heat effects are a result of other equilibria like structural changes, self-assembly, or both. Since to date no data are available on the structure of full-length HMGB1 in solution that could assist us to find a more suitable binding model, we also fitted these binding isotherms with a noncooperative binding model. However, as a consequence, the reported binding constants and thermodynamic parameters report apparent rather than intrinsic values. A working hypothesis that would explain the observed calorimetric and spectroscopic data measured on HMGB1 is presented under Discussion.

RESULTS

The polypeptides used in this study are shown in Figure 1, and were purified as described under Materials and Methods.

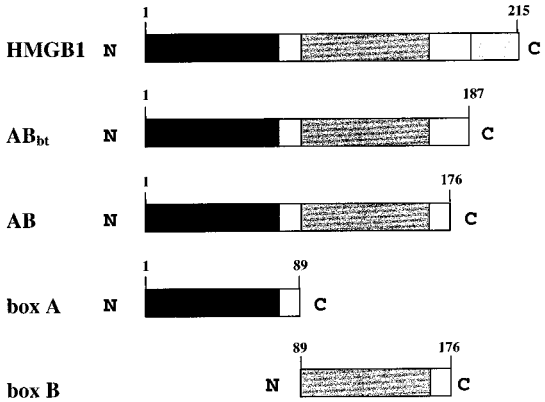

FIGURE 1: Schematic representation of the proteins used in this study. Numbers indicate the expressed amino acids. HMG box A is drawn in black, HMG box B in gray. The 30 amino acids comprising the acidic tail of HMGB1 are indicated with gray bars. White areas show basic linker regions.

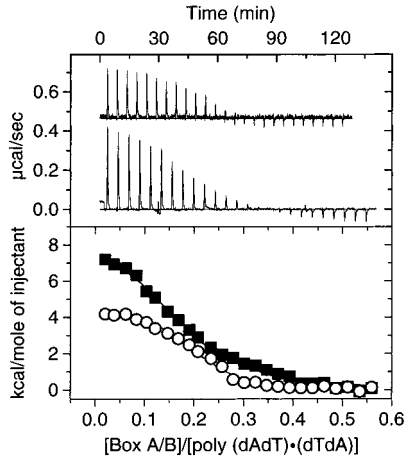

FIGURE 2: Experimental calorimetric data of the binding of box A and box B to poly-AT duplex DNA. Titrations were performed at 15 °C. The top panel shows the raw heat data obtained over a series of injections of poly-AT into box A (upper curve) and box B (lower curve). Dilution heats measured by titrating poly-AT into the corresponding buffer were in the range of the heat effects observed at the end of the titration (not shown). The integrated heat signals of the data shown in the top panel of the figure gave rise to the binding isotherm shown in the lower panel. The solid line represents a calculated curve using the best-fit parameters obtained by a nonlinear least-squares fit. Integrated heat signals measured using box B are shown as solid squares, and those using box A are shown as open circles. To make figures comparable, all ITC data were displayed as reverse titration showing binding heats on the *y*-axis and the ratio [protein/DNA] on the *x*-axis.

Binding of the Single Boxes A and B to Duplex DNA. The thermodynamics of the interaction of the single HMG boxes A and B with duplex DNA were analyzed using isothermal titration calorimetry. In the temperature interval used for binding studies (10−27 °C), HMGB1 has been reported to be completely folded (*12*). In the experiments performed, DNA was titrated into a solution of box A or box B, respectively. The binding isotherm is characterized by an initial strong heat uptake that decreases when the binding sites on DNA become saturated. In the last injections of each titration, only dilution heat effects were observed. Figure 2 shows the heat effects of 25 subsequent injections of poly-AT into solutions of box A and box B, respectively. A nonlinear least-squares fit of the binding curves provided values for the number of base pairs covered upon association

Table 1: Binding of Single HMGB1 Boxes to Duplex DNA

T (°C)	ΔH_{obs} (kcal/mol)	$T\Delta S_{obs}$ (kcal/mol)	ΔG_{obs} (kcal/mol)	$K_{B,obs}$ ($\times 10^6$ M^{-1})	n_{obs}	no. of expts
			Box A Binding to Poly-AT			
15	4.7 ± 0.3	12.7 ± 0.4	−8.0 ± 0.4	1.2 ± 0.4	4.9 ± 0.5	5
			Box A Binding to Poly-GC			
15	2.4 ± 0.7	10.5 ± 0.5	−8.1 ± 0.2	1.3 ± 0.6	5.3 ± 0.4	2
			Box B Binding to Poly-AT			
15	8.3 ± 0.6	16.9 ± 0.4	−7.5 ± 0.2	0.5 ± 0.15	5.5 ± 0.4	3
			Box B Binding to Poly-GC			
15	3.8 ± 0.4	10.9 ± 0.4	−7.1 ± 0.4	0.3 ± 0.15	4.9 ± 0.5	2

Table 2: Binding of AB and AB_{bt} to Duplex DNA

T (°C)	ΔH_{obs} (kcal/mol)	$T\Delta S_{obs}$ (kcal/mol)	ΔG_{obs} (kcal/mol)	$K_{B,obs}$ ($\times 10^6$ M^{-1})	n_{obs}	no. of expts
			AB Binding to Poly-AT			
15	17.1 ± 3.0	24.9 ± 2.5	−7.8 ± 0.5	2.9 ± 0.5	11.9 ± 0.2	5
			AB Binding to Poly-GC			
15	14.1 ± 0.5	22.9 ± 0.3	−8.8 ± 0.5	3.9 ± 0.5	10.0 ± 0.1	2
			AB_{bt} Binding to Poly-AT			
15	21.8 ± 0.3	30.0 ± 0.3	−8.2 ± 0.3	1.9 ± 0.3	15.4 ± 0.5	2
			AB_{bt} Binding to Poly-GC			
15	28.7 ± 0.8	37.8 ± 0.8	−9.1 ± 0.8	8.5 ± 0.7	10.0 ± 0.1	2

(n_{obs}), the equilibrium constant ($K_{B,obs}$), and the change in enthalpy (ΔH_{obs}). The binding of box A to poly-AT at 15 °C is characterized by $K_{B,obs} = (1.2 \pm 0.4) \times 10^6$ M^{-1}, $\Delta H_{obs} = 4.7 \pm 0.3$ kcal/mol, and $n_{obs} = 4.9 \pm 0.3$ (Table 1). Comparable affinity and binding thermodynamic equilibrium parameters have been obtained for binding to poly-GC, with a slightly smaller heat uptake of 2.4 ± 0.7 kcal/mol (Table 1).

As already observed in the case of measurements carried out using box A, also binding of box B to duplex DNA was found to be unspecific, and similar affinity constants were determined for poly-AT and poly-GC [$(0.5 \pm 0.15) \times 10^6$ M^{-1} and $(0.3 \pm 0.2) \times 10^6$ M^{-1}, respectively]. Also in this case, binding is an entropically driven process, but the unfavorable binding enthalpy is considerably larger (8.3 ± 0.6 and 4.7 ± 0.3 kcal/mol for box B and box A, respectively). The affinity of box B to duplex DNA was found to be about 3 times lower when compared to box A. Using poly-GC as a substrate, binding of box B was less enthalpically unfavorable than to poly-AT.

Binding of AB and AB_{bt} to Duplex DNA. Combining the two HMG boxes in the construct AB (residues 1−176) resulted in an increase in binding affinity [$(2.9 \pm 0.5) \times 10^6$ M^{-1} and $(3.9 \pm 0.5) \times 10^6$ M^{-1}, for poly-AT and poly-GC, respectively; Table 2]. Binding enthalpy changes measured at 15 °C using AB were large and positive for both poly-AT and poly-GC (Table 2). However, binding to poly-GC showed an about 3 kcal/mol less unfavorable enthalpy contribution to the binding free energy change than observed in the case of poly-AT.

The two HMG boxes in HMGB1 are linked with a stretch of basic amino acids with the C-terminal acidic tail. The importance of these linker residues for binding to DNA has been pointed out in the case of the *Drosophila* protein HMG-D (*28*) as well as HMGB1/2 (*29*−*31*). The construct AB was therefore prolonged to include the entire basic tail (AB_{bt}). AB_{bt} binding to poly-AT occurred with similar affinity and in an essential noncooperative way (Table 2). The binding site covered upon binding was found to be larger than in the case of AB ($n_{obs} = 15.4 \pm 0.5$ versus 11.9 ± 0.2). At 15 °C, binding enthalpy changes were large and positive and about 3 kcal/mol more unfavorable than in the case of AB. AB_{bt} bound with about 2-fold higher affinity to poly-GC than AB. The binding is also noncooperative and strongly opposed by enthalpy (28.7 kcal/mol).

Binding of Full-Length HMGB1 to Duplex DNA. Binding of full-length HMGB1 to duplex DNA showed a number of very interesting features, in particular when poly-AT was used as a substrate. Direct titration experiments (titrating poly-AT into HMGB1) gave rise to a more complex binding isotherm with a curvature typically observed for ligands with positive binding cooperativity (Figure 3A). These additional heat effects at high saturation levels of this model DNA were observed in all experiments using poly-AT and full-length HMGB1. Also in reverse titrations (titrating HMGB1 into poly-AT), small additional heat effects were observed when the lattice was almost completely saturated (Figure 3B).

However, we did not succeed in improving the quality of the nonlinear least-squares fits using a model in which a cooperativity parameter (ω) was included, and values for ω remained around 1. As a consequence, the reported binding constants and thermodynamic parameters for the binding of full-length HMGB1 to poly-AT have to be considered as apparent rather than intrinsic binding constants. Noncooperative binding was observed using poly-GC, and the measured data could be represented well by the noncooperative binding model (Figure 3C).

Comparing binding of full-length HMGB1 to the two model substrates, a second very interesting aspect is the small positive binding enthalpy of only 4.3 ± 0.5 kcal/mol at 15 °C observed using poly-GC. It is interesting to note that this enthalpy change is similar to the one measured using only a single HMG box. On the other hand, binding of AB to poly-GC results in a large positive enthalpy change of 14.1 ± 0.5 kcal/mol. Using poly-AT as a substrate, apparent binding enthalpy changes were comparable to those determined for AB and AB_{bt}, respectively.

Finally, binding of full-length HMGB1 to poly-AT and poly-GC differed also significantly in the observed binding site length. Using poly-AT, the observed binding site length increased steadily with increasing size of the protein from 4.9 ± 0.5 for a single box to 11.9 ± 0.2 for AB, 15 ± 0.5 for AB_{bt}, and 19 ± 1 for full-length HMGB1, whereas in measurements where poly-GC was used the apparent binding site size remained constant for AB, AB_{bt}, and the full-length protein.

Thus, thermodynamic data measured on the binding of different HMGB1 constructs to the different types of model duplex DNA (poly-AT and poly-GC) clearly indicate that truncated versions of HMGB1 have different binding properties in solution than the full-length protein. In addition, binding of full-length HMGB1 to G/C-rich sequences differs significantly from binding to A/T-rich sequences in binding enthalpy, binding constants, and binding site size. Modulation of binding characteristics by the acidic tail also becomes apparent when comparing binding affinities to poly-AT and poly-GC. Whereas AB_{bt} binds poly-GC with higher affinity than poly-AT, the opposite is the case for the full-length protein.

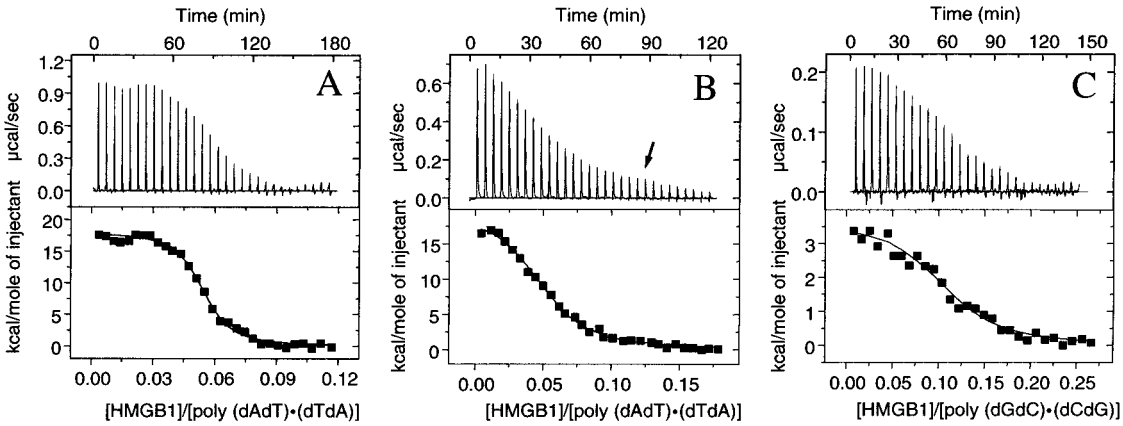

FIGURE 3: ITC data of the binding of full-length HMGB1 to duplex DNA. Shown are a titration (A) and a reverse titration (B) using poly-AT as well as a titration using poly-GC (C). The figure has been generated in the same way as described in the legend of Figure 2. A noncooperative binding model was used to fit data. However, binding cooperativity is obvious in (A). An arrow indicates the small additional heat effects as a result of binding cooperativity in (B). Binding to poly-GC is clearly noncooperative. The results of the least-squares fits are summarized in Table 3.

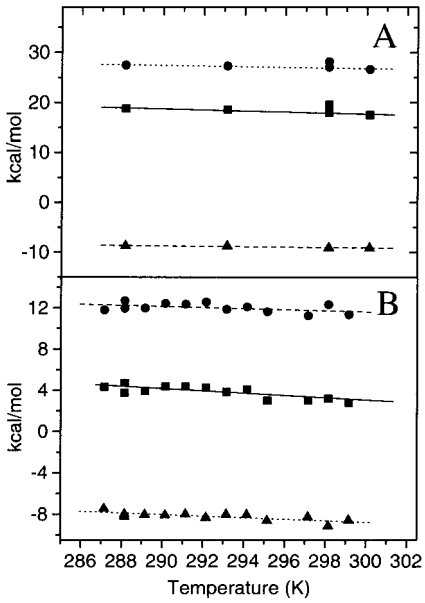

FIGURE 4: Temperature dependence of the determined thermodynamic parameters. (A) Changes in binding enthalpy (■), entropy ($T\Delta S$) (●), and free energy (▲) upon binding of full-length HMGB1 to poly-AT as functions of temperature as well as linear least-squares fits of these data. (B) Temperature dependence of the measured thermodynamic parameter of box A binding to poly-AT. Identical symbols have been used as in Figure 4A.

Temperature Dependence of ΔH_{obs} upon Binding of Box A and HMGB1. Enthalpy changes upon binding of full-length HMGB1 and box A to poly-AT were only weakly temperature dependent (Figure 4, and Table 3). From the slopes of the temperature dependence of the binding enthalpies, a heat capacity change of -0.13 ± 0.02 kcal mol^{-1} K^{-1} and of -0.10 ± 0.05 kcal mol^{-1} K^{-1} was determined for box A and full-length HMGB1, respectively. The temperature dependence was essentially linear with an R-value of 0.95 for full-length HMGB1 and 0.82 for box A. ΔG_{obs} decreases slightly with increasing temperature by 43 ± 10 and 75 ± 15 cal mol^{-1} K^{-1} per degree for full-length HMGB1 and box A, respectively.

CD Spectra. CD spectroscopy was used to detect structural changes in DNA upon binding of full-length HMGB1 and its single boxes A and B (Figure 5). In the region between 245 and 300 nm, CD spectra of DNA were not significantly affected by the spectral contribution of the protein, and the recorded spectra therefore report structural changes of the DNA only.

Table 3: Binding of Full-Length HMGB1 to Duplex DNA

T (°C)	ΔH_{obs} (kcal/mol)	$T\Delta S_{obs}$ (kcal/mol)	ΔG_{obs} (kcal/mol)	$K_{B,obs}$ ($\times 10^6$ M^{-1})	n_{obs}	no. of expts
Full-Length HMGB1 Binding to Poly-AT (Titration)[a]						
15	18.8 ± 0.3	27.5 ± 0.5	-8.6 ± 0.5	3.5 ± 0.7	20.8 ± 0.6	3
20	18.6 ± 0.3	27.3 ± 0.3	-8.7 ± 0.3	2.9 ± 0.3	18.2 ± 0.4	1
25	18.0 ± 0.2	27.1 ± 0.4	-9.1 ± 0.4	4.4 ± 0.5	18.1 ± 0.4	1
27	17.5 ± 0.3	26.6 ± 0.6	-9.1 ± 0.6	4.3 ± 0.8	18.0 ± 0.5	1
Full-Length HMGB1 Binding to Poly-AT (Reverse Titration)[a]						
20	18.8 ± 0.3	26.9 ± 0.3	-8.1 ± 0.3	1.0 ± 0.2	21.0 ± 0.6	2
25	19.6 ± 0.4	28.2 ± 0.4	-8.5 ± 0.3	1.1 ± 0.4	19.3 ± 0.5	1
Full-Length HMGB1 Binding to Poly-GC (Titration)						
15	4.3 ± 0.5	11.7 ± 0.3	-7.4 ± 0.3	0.5 ± 0.3	9.8 ± 0.4	2

[a] Binding isotherms of full-length HMGB1 to poly-AT have been fitted using a noncooperative binding model. As a consequence, the reported binding constants are therefore apparent and not intrinsic binding constants (see text).

The CD spectrum of poly-AT is characterized by a strong negative signal at 247 nm and a broad maximum around 265 nm (Figure 5A). Upon saturation with full-length HMGB1 or with the single boxes A or B, the maximum at 265 nm is blue-shifted (262 nm) and the CD signal is reduced between 262 and 300 nm. We observed no large differences between full-length HMGB1 and its C-terminally truncated versions. Changes observed in the CD spectra of poly-AT upon saturation with HMGB1 occurred already at low saturation levels (10%) and did not change significantly when more binding sites were occupied by full-length HMGB1 (Figure 5B).

The CD spectra of poly-GC showed a strong negative signal at 252 nm and a broad maximum around 273 nm with a shoulder at 287 nm (Figure 5C). The CD spectra of poly-GC did not change significantly upon saturation with box A, which resulted only in a slight reduction of the measured CD signal between 270 and 300 nm. Interestingly, binding of full-length HMGB1 and box B led to a significant increase of the CD signal at 285 nm. In addition, the maximum at 273 nm is red-shifted. The similarity of the CD spectra obtained with full-length HMGB1 and box B suggests that

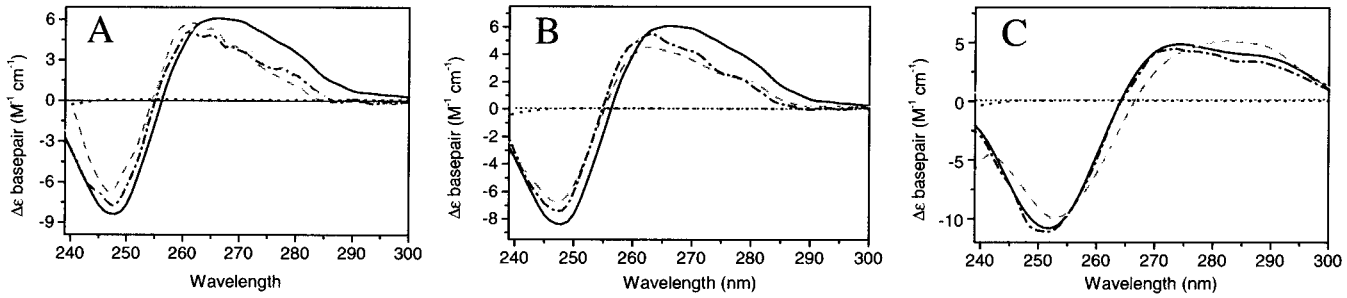

FIGURE 5: CD spectra monitoring conformational changes in DNA upon saturation with HMGB1 and its single domains. (A) Spectral changes upon binding of HMGB1 and box A/B to poly-AT. Shown are spectra of poly-AT (straight line), full-length HMGB1 only (dotted line), poly-AT saturated with box A (dash−dot line), poly-AT saturated with box B (gray dashed line), and poly-AT saturated with full-length HMGB1 (light gray short dashed line). (B) Dependency of the CD spectra of poly-AT (straight line) on the level of saturation with full-length HMGB1. Shown are spectra with saturation levels of 10% (gray dashed line), 50% (light gray short dashed line), and 100% (dash−dot line) and full-length HMGB1 only (dotted line). (C) Spectral changes upon binding of HMGB1 and box A/B to poly-GC. Shown are spectra of poly-GC (straight line), full-length HMGB1 only (dotted line), poly-GC saturated with box A (dash−dot line), poly-GC saturated with box B (gray dashed line), and poly-GC saturated with full-length HMGB1 (light gray short dashed line).

the structural changes of this model DNA induced upon binding of these two proteins are similar, and differ from those induced upon binding of box A.

DISCUSSION

Considerable numbers of structural and thermodynamic studies have been carried out in recent years in order to characterize the binding of sequence-specific DNA binding proteins. In contrast, thermodynamic studies of non-sequence-specific DNA binding proteins have rarely been reported due to the difficulties in studying those systems (*32, 33*). Several groups have circumvented the problems concerning non-sequence-specific binding by using small oligonucleotides that are only able to accommodate one protein molecule. However, such an analysis still assumes that binding at different positions on this small DNA stretch is thermodynamically identical, an assumption that is unlikely to be met in reality because of end-effects. Previous studies on DNA binding affinities of HMGB1 or HMG boxes to double-stranded DNA have used DNA mobility shift assays or surface plasmon resonance (SPR) measurements (*17, 34*−*36*). Binding affinities obtained using the latter method differed considerably depending on the surface of the chip used to immobilize the oligonucleotides, and range from $K_D = 4.3 \times 10^{-6}$ M using a charged matrix to $K_D = 2.01 \times 10^{-8}$ M using a hydrophobic matrix (*31, 37*).

In the present study, we have characterized the binding of HMGB1 to long DNA stretches in solution using isothermal titration calorimetry. Our analysis of the binding isotherms assumes that the observed binding heats are proportional to the binding density. In calorimetric measurements, the observed heat signal originates from all binding events. However, different binding modes that are energetically similar or that occur with enthalpy changes close to 0 may exist. The determined thermodynamic data are therefore only valid assuming that the above-mentioned assumption is true. Self-association of the protein boxes A and B as well as AB and AB_{bt} in solution was ruled out using analytical ultracentrifugation experiments that showed that these proteins are entirely monomeric under the solvent conditions used (data not shown).

We have chosen the two B-DNA substrates poly-AT and poly-GC as a model system for the binding of HMGB1 and its truncated derivatives to A/T- and G/C-rich linear duplex DNA. These long DNA substrates minimize problems such as structural fluctuations due to fraying of end base pairs, common to small double-stranded oligonucleotides. In addition, longer DNA stretches allow the detection of cooperativity. The theoretical aspects of cooperative and noncooperative binding of nonspecific DNA binding proteins have been elaborated a considerable time ago (*26*). It is therefore surprising that these models have only rarely been used in practical applications using titration calorimetry (*32, 33*). Using the McGee and von Hippel model for the calculation of binding affinities in solution, we find that the affinities of HMGB1 for duplex DNA (Table 3) lie between the extreme values reported for SPR studies using either a hydrophilic or a hydrophobic grid (*31, 37*). Dissociation constants for full-length HMGB1 binding to linear duplex DNA are in the low micromolar range and are considerably larger than dissociation constants of sequence-specific HMG box proteins; for example, the HMG box in Sox5 binds with 2.5×10^{-8} M affinity (*38*).

HMGB1 binds to highly bent DNA substrates such as four-way junctions and cisplatin-modified DNA with dissociation constants in the range of 10^{-8}−10^{-9} M (*15*−*17*). However, these distorted DNA forms occur only rarely in the cell, and the main biological role of HMGB1 must involve binding to B-DNA. The concentration of HMGB1 in mammalian nuclei is in the micromolar range, and furthermore HMGB1 interacts with several DNA binding proteins that are likely to recruit it to DNA. Thus, the binding affinity of HMGB1 for linear DNA is probably sufficient to engage a significant fraction of the HMGB1 pool with B-DNA in vivo.

A typical thermodynamic feature of nonspecific DNA binding is the small heat capacity change ($\Delta C_{p,obs}$) that occurs upon association (*39, 40*). Also in the case of HMGB1 a very small heat capacity difference of -0.10 ± 0.05 kcal mol^{-1} K^{-1} for full-length HMGB1 and -0.13 ± 0.02 kcal mol^{-1} K^{-1} for box A was determined, whereas binding of the sequence-specific HMG box in mouse Sox-5 to its recognition sequence gave rise to a heat capacity change of -0.956 kcal mol^{-1} K^{-1} (*38*). $\Delta C_{p,obs}$ is related to the change in solvent-exposed surface area upon complex formation (*41*−*43*). Unfortunately, no structural information is available for a complex of HMGB1 with unmodified duplex DNA. However, comparing $\Delta C_{p,obs}$ of full-length HMGB1 and box A indicates that a simple surface area relation is not obvious,

since full-length HMGB1 is expected to cover a significantly larger surface area upon binding than box A alone.

Single HMG boxes bind to DNA with affinities close to 10^{-6} M and occupy about 5 base pairs. As expected, the boxes have no affinity preference for poly-AT or poly-GC. Box A binds much more tightly to linear duplex DNA than box B. The weaker affinity of box B for double-stranded DNA is a result of the larger unfavorable binding enthalpies. In addition, binding enthalpies for box A and B are larger using poly-AT than poly-GC.

The covalent linkage of the single boxes in AB results in the doubling of the size of the binding site. The binding affinity for DNA also increases with respect to single boxes, but not as much as expected for a bidentate versus a monodentate binding mode. Furthermore, the basic region that flanks box B has been reported to enhance DNA binding, supercoiling, and bending activities (*44*). However, for poly-AT, we did not observe an increase in binding affinity for AB_{bt}, that contains the entire basic region flanking the B domain, but simply an increase in size of the apparent binding site by about 3 base pairs. Using poly-GC, the affinity increased about 2-fold when compared to AB.

The presence of the acidic tail in full-length HMGB1 modulates significantly its binding properties for duplex DNA. Our studies on full-length HMGB1 reveal significant differences in binding to poly-AT and poly-GC. Particularly, there are significant differences in the apparent binding site size, binding enthalpy, and cooperativity.

Binding isotherms measured using poly-AT as model DNA revealed a more complex association behavior. The observed curvature of the binding isotherms is typically observed for cooperative binding of ligands. Likewise, positive cooperativity has been observed for a number of nonspecific DNA binding proteins including the single-strand binding protein SSB (*45*) as well as the bacteriophage T4 gene 32 and 5 proteins (*46*).

Cooperativity is a thermodynamic parameter that reflects the influence of one bound ligand on the binding affinity of a second, and is a result of protein−protein interactions and/or short-range conformational changes that are induced in the DNA upon binding of a ligand. However, we did not succeed in determining the cooperativity parameter (ω) using a cooperative binding model (*26*). Thus, probably the molecular events that take place upon association of full-length HMGB1 with poly-AT are not compatible with this binding model. From the data presented here and those published earlier, we can speculate on the mechanisms of the binding of HMGB1 to poly-AT and poly-GC. First, the observed additional heat effects require the presence of the acid tail, since they were absent in measurements using AB and AB_{bt}. It has been demonstrated earlier that the C-terminal acidic tail modulates an intramolecular conformational change involving SH groups within HMGB1 (*13*). In addition, a calorimetric analysis of the melting behavior of the single domains, AB, and full-length HMGB1 demonstrated that the acidic tail interacts with one of the boxes, stabilizing the interacting domain by about 2.5 kcal/mol, whereas the noninteracting domain is destabilized (*12*). The tail−box interaction may occur between molecules, as well as intramolecularly. A recent sedimentation velocity analysis has shown that the predominant form of HMGB1 in solution is monomeric, but about 7% exists as dimers (*47*). Due to the high effective concentration of HMGB1 on DNA at saturation, the weak interaction that can be measured in solution will be very effective on a monodimensional lattice. Thus, the observed additional heat effects arise most likely as a result of a direct interaction between different HMGB1 molecules that stabilize complex formation.

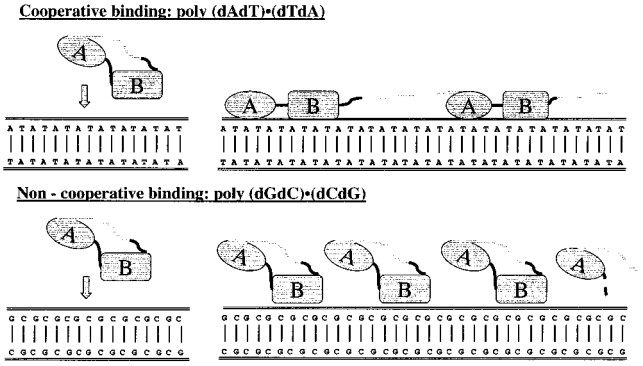

FIGURE 6: Model of the mechanisms of HMGB1 binding to poly-AT and poly-GC. The number of base pairs covered by the two DNA binding domains correspond to those measured in the ITC experiments. For reasons of simplicity, the bending of DNA upon binding has not been considered. The acidic tail of HMGB1 is shown as a gray line. For details of the figure, see description in the text.

No cooperativity has been observed using poly-GC. Thus, in this case, the acidic tail does not interact with its nearest neighbor on the linear DNA but interacts most likely intramolecularly with one of the boxes. In addition, the binding site size does not increase when the construct AB is extended further. CD data indicate that conformational changes in poly-GC upon binding of full-length HMGB1 are similar to those observed for domain B alone. We propose that when full-length HMGB1 binds to poly-GC, only domain B is in contact with the DNA, while box A remains blocked by the acidic tail. This hypothesis is supported by similar binding enthalpies measured for box B and full-length HMGB1. When binding to A/T-rich sequences such as poly-AT, the intermolecular interaction of the tail is disrupted and both boxes bind the DNA. The tail is free to interact with the neighboring box A, resulting in the observed cooperativity and the larger apparent binding site size.

Taking these data together, the following mechanisms of HMGB1 binding to linear duplex DNA can be envisioned. We postulate that in solution the acidic tail interacts with domain A. In the case of an already distorted DNA structure like a four-way junction or cisplatinated DNA as a substrate, box A binds directly to this high-affinity site whereas box B binds to the adjacent double-stranded DNA. When the substrate is a linear DNA strand, domain B binds first and bends strongly the double helix by intercalation of several residues. Box A binds next and thereby releases the acidic tail. This second binding event, however, occurs only when the DNA substrate is easily distorted, as is the case for A/T-rich sequences. More rigid DNA forms such as G/C-rich sequence stretches are only bound by box B. The postulated model is depicted in Figure 6.

The tail by itself does not interact with DNA, but can alter the binding properties. Depending on the flexibility of the target DNA site, one or both HMG domains interact with DNA. In the two different binding modes, the acidic tail is either released or still interacts with box A. Once released,

the acidic tail may also interact with neighboring molecules such as histones or transcription factors. This sequence-dependent binding of HMGB1 is likely to have functional significance, as some sequence specificity has been reported for HMGB1 in enhanceosome assembly (*48*).

Within the family of nonspecific HMG proteins, HMGB1 has the longest acidic tail (30 amino acids) and HMGB3 the shortest (24 amino acids). The length and the sequence of the tail are extremely conserved across species. Because of the larger size, the tail of HMGB1 should reach further than that of HMGB3, providing differences in DNA and protein binding preferences between the two proteins.

Even though the proposed mechanisms of HMGB1 binding to duplex DNA need to be confirmed by further studies, they explain readily the measured calorimetric and spectroscopic data and offer an explanation both for the duplication of the HMG domain (whereas only a single box is present in yeast and plant HMG-like molecules) and for the presence (and tight evolutionary conservation) of the acidic tail in vertebrates. It has been pointed out that the efficiency of HMGB1 in inducing looping and supercoiling is modulated by its acidic tail: its presence results in a 4−5-fold reduction in both DNA binding affinity and supercoiling ability (*13*, *14*). In the *Drosophila* homologue HMG-D, the acidic tail modulates the structural selectivity of DNA binding (*28*). Our studies confirm and extend the function of the acidic tail in modulating DNA binding by HMG proteins.

ACKNOWLEDGMENT

We thank Prof. J. Thomas for the generous gift of plasmid pT7-7-rHMG1cm, T. Bonaldi for initial help in protein purification, and Dr. T. Lundbäck for providing us with the Mathematica fitting routines.

REFERENCES

1. Baxevanis, A. D., and Landsman, D. (1995) *Nucleic Acids Res. 23*, 1604−1613.
2. Bianchi, M. E., and Beltrame, M. (2000) *EMBO Rep. 1*, 109−114.
3. Bustin, M. (1999) *Mol. Cell. Biol. 19*, 5237−5246.
4. Giese, K., Amsterdam, A., and Grosschedl, R. (1991) *Genes Dev. 5*, 2567−2578.
5. Goodfellow, P. N., and Lovell-Badge, R. (1993) *Annu. Rev. Genet. 27*, 71−92.
6. Grosschedl, R., Giese, K., and Pagel, J. (1994) *Trends Genet. 10*, 94−100.
7. Bustin, M. (2001) *Trends Biochem. Sci. 26* (3), 152−153.
8. Travers, A. (2000) *Curr. Opin. Struct. Biol. 10*, 102−109.
9. Murphy, F. V., IV, and Churchill, M. E. (2000) *Struct. Folding Des. 8*, R83−89.
10. Hill, D. A., Pedulla, M. L., and Reeves, R. (1999) *Nucleic Acids Res. 27*, 2135−2144.
11. Webb, M., and Thomas, J. O. (1999) *J. Mol. Biol. 294*, 373−387.
12. Ramstein, J., Locker, D., Bianchi, M. E., and Leng, M. (1999) *Eur. J. Biochem. 260*, 692−700.
13. Sheflin, L. G., Fucile, N. W., and Spaulding, S. W. (1993) *Biochemistry 32*, 3238−3248.
14. Stros, M., Stokrová, J., and Thomas, J. O. (1994) *Nucleic Acids Res. 22*, 1044−1051.
15. Bianchi, M. E., Beltrame, M., and Paonessa, G. (1989) *Science 243*, 1056−1059.
16. Ohndorf, U. M., Rould, M. A., He, Q., Pabo, C. O., and Lippard, S. J. (1999) *Nature 399*, 708−712.
17. Pil, P. M., and Lippard, S. J. (1992) *Science 256*, 234−236.
18. Aidinis, V., Bonaldi, T., Beltrame, M., Santagata, S., Bianchi, M. E., and Spanopoulou, E. (1999) *Mol. Cell. Biol. 19*, 6532−6542.
19. van Gent, D. C., Hiom, K., Paull, T., and Gellert, M. (1997) *EMBO J. 16*, 2665−2670.
20. Paull, T. T., Haykinson, M. J., and Johnson, R. C. (1993) *Genes Dev. 7*, 1521−1534.
21. Calogero, S., Grassi, F., Aguzzi, A., Voigtländer, T., Ferrier, P., and Bianchi, M. E. (1999) *Nat. Genet. 22*, 276−280.
22. Allain, F. H., Yen, Y. M., Masse, J. E., Schultze, P., Dieckmann, T., Johnson, R. C., and Feigon, J. (1999) *EMBO J. 18*, 2563−2579.
23. Bianchi, M. E., Falciola, L., Ferrari, S., and Lilley, D. M. J. (1992) *EMBO J. 11*, 1055−1063.
24. Bianchi, M. E. (1991) *Gene 104*, 271−275.
25. Gill, S. C., and von Hippel, P. H. (1989) *Anal. Biochem. 182*, 319−326.
26. McGhee, J. D., and von Hippel, P. H. (1974) *J. Mol. Biol. 86*, 469−489.
27. Lohman, T. M., and Mascotti, D. P. (1992) *Methods Enzymol. 212*, 400−424.
28. Payet, D., and Travers, A. A. (1996) *J. Mol. Biol. 266*, 66−75.
29. Saito, K., Kikuchi, T., Shirakawa, H., and Yoshida, M. (1999) *J. Biochem. (Tokyo) 125*, 399−405.
30. Stros, M. (1998) *J. Biol. Chem. 273*, 10355−10361.
31. Yamamoto, A., Ando, Y., Yoshioka, K., Saito, K., Tanabe, T., Shirakawa, H., and Yoshida, M. (1997) *J. Biochem. (Tokyo) 122*, 586−594.
32. Lundback, T., Hansson, H., Knapp, S., Ladenstein, R., and Härd, T. (1998) *J. Mol. Biol. 276*, 775−786.
33. McAfee, J. G., Edmondson, S. P., Zegar, I., and Shriver, J. W. (1996) *Biochemistry 35*, 4034−4045.
34. Falciola, L., Murchie, A. I. H., Lilley, D. M. J., and Bianchi, M. E. (1994) *Nucleic Acids Res. 22*, 285−292.
35. Kasparkova, J., Farrell, N., and Brabec, V. (2000) *J. Biol. Chem. 275*, 15789−15798.
36. Wagner, J. P., Quill, D. M., and Pettijohn, D. E. (1995) *J. Biol. Chem. 270*, 7394−7398.
37. Webster, C. I., Cooper, M. A., Packman, L. C., Williams, D. H., and Gray, J. C. (2000) *Nucleic Acids Res. 28*, 1618−1624.
38. Privalov, P. L., Jelesarov, I., Read, C. M., Dragan, A. I., and Crane-Robinson, C. (1999) *J. Mol. Biol. 294*, 997−1013.
39. Oda, M., Furukawa, K., Ogata, K., Sarai, A., and Nakamura, H. (1998) *J. Mol. Biol. 276*, 571−590.
40. Tanha, J., and Lee, J. S. (1997) *Nucleic Acids Res. 25*, 1442−1449.
41. Gill, S. J., Dec, S. F., Olofsson, G., and Wadsö, I. (1985) *J. Phys. Chem. 89*, 3758−3761.
42. Murphy, K. P., and Freire, E. (1992) *Adv. Protein. Chem. 43*, 313−361.
43. Spolar, R. S., and Record, M. T., Jr. (1994) *Science 263*, 777−784.
44. Teo, S.-H., Grasser, K. D., and Thomas, J. O. (1995) *Eur. J. Biochem. 230*, 943−950.
45. Lohman, T. M., Overman, L. B., and Datta, S. (1986) *J. Mol. Biol. 187*, 603−615.
46. Kowalczykowski, S. C., Lonberg, N., Newport, J. W., and von Hippel, P. H. (1981) *J. Mol. Biol. 145*, 75−104.
47. Ranatunga, W., Lebowitz, J., Axe, B., Pavlik, P., Kar, S. R., and Scovell, W. M. (1999) *Biochim. Biophys. Acta 1432*, 1−12.
48. Ellwood, K. B., Yen, Y. M., Johnson, R. C., and Carey, M. (2000) *Mol. Cell. Biol. 20*, 4359−4370.

BI0100900